2015

FINITE VOLUME METHODS FOR LINEAR PARTIAL DIFFERENTIAL EQUATIONS WITH DELTA-SINGULARITIES

Nattaporn Chuenjarern
Michigan Technological University

FINITE VOLUME METHODS FOR LINEAR PARTIAL DIFFERENTIAL EQUATIONS WITH DELTA-SINGULARITIES

By

Nattaporn Chuenjarern

A REPORT

Submitted in partial fulfillment of the requirements for the degree of

MASTER OF SCIENCE

In Mathematical Sciences

MICHIGAN TECHNOLOGICAL UNIVERSITY

2015

This report has been approved in partial fulfillment of the requirements for the Degree of MASTER OF SCIENCE in Mathematical Sciences.

Department of Mathematical Sciences

Report Advisor: *Dr. Yang Yang*

Committee Member: *Dr. Zhengfu Xu*

Committee Member: *Dr. Kuilin Zhang*

Department Chair: *Dr. Mark S. Gockenbach*

Contents

List of Figures

List of Tables

Acknowledgements

Abstract

In this work, we study hyperbolic conservation law in one space dimension with δ-singularities as the initial data. We use finite volume methods to find the sizes of pollution region. Firstly, we study finite volume method (FVM) with linear weights and weighted essentially non-oscillatory (WENO) scheme and apply both methods to linear partial differential equations without singularities to check the accuracy. Then we use both methods to find the numerical solutions and compute errors of linear equations with δ-singularities. Lastly, we use such results to find the size of pollution region of each method. These results show that the size of the pollution region is approximately of the order $O(\Delta x^{1/2})$, where Δx is the spatial mesh size.

Chapter 1

Introduction to hyperbolic conservation laws

In this chapter, we will introduce some information about the hyperbolic conservation laws.

The following first-order partial differential equation

$$u_t + f(u)_x = 0 \tag{1.1}$$

is called a *hyperbolic conservation law* in one dimensional space. $u = u(x,t)$ is the *conserved quantity*, f is the *flux*, t and x are the *time* and *spatial* variables, respectively.

Hyperbolic conservation laws can be used to model many transport phenomena. Given interval $[a, b]$, we integrate (1.1) over the interval to obtain

$$\int_a^b u_t(x,t)dx + \int_a^b f(u(x,t))_x dx = 0,$$

$$\frac{d}{dt}\int_a^b u(x,t)dx = -\int_a^b f(u(x,t))_x dx$$

$$= f(u(a,t)) - f(u(b,t))$$

$$= [\text{inflow at a}] - [\text{outflow at b}].$$

In other words, the total amount of u contained inside an interval $[a, b]$ is chang-
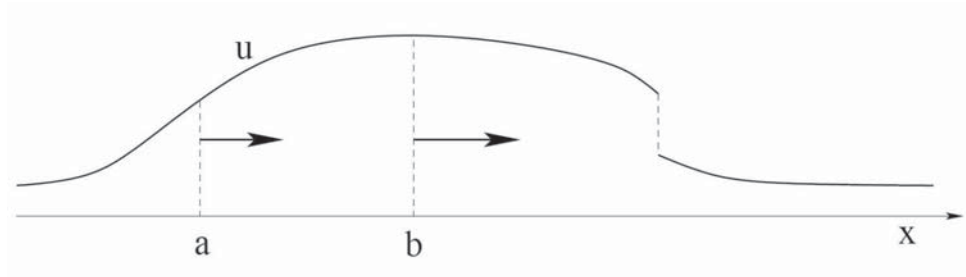
Figure 1.1: Flow across two points.

ing according to the flow of u across boundary points.

Next, we will give an example of hyperbolic conservation law described in [1].
Example 1 (Traffic flow) Let $u(x, t)$ be the density of cars on a highway at the point x time t. This can be measured as the number of cars per kilometer (see Figure 1.2). We assume that u is continuous and the speed s of the cars depends only on their density, say $s = s(u)$ with $\frac{ds}{du} < 0$. Given any two points a, b on the highway, the number of cars between a and b therefore varies according to (1.1).
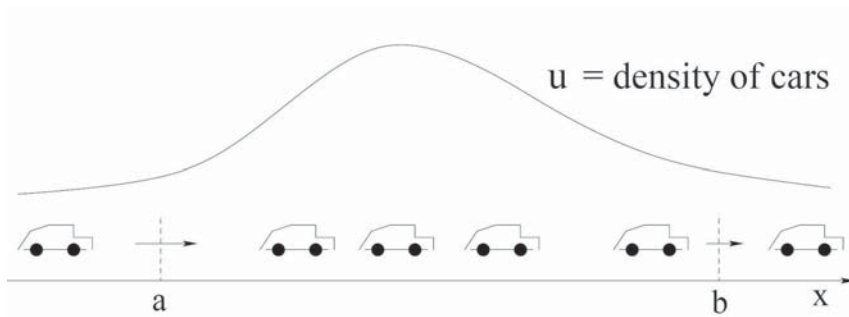
Figure 1.2: The density of cars can be described by a conservation law.

2

$$\int_a^b u_t(x,t)dx = \frac{d}{dt}\int_a^b u(x,t)dx$$

$$= [\text{inflow at a}] - [\text{outflow at b}]$$

$$= s(u(a,t)) \cdot u(a,t) - s(u(b,t)) \cdot u(b,t)$$

$$= -\int_a^b [s(u)u]_x dx.$$

Since the above equation holds for all a, b, it yields the conservation law in one dimensional space:

$$u_t + [s(u)u]_x = 0,$$

where u is the conserved quantity and $f(u) = s(u)u$ is the flux function.

Chapter 2

The algorithm of the finite volume schemes

In this section we will describe the finite volume methods with linear weights and WENO scheme.

2.1 Finite Volume Scheme

First of all, we introduce some basic idea of finite volume scheme explained in [3] and [4]. Consider the hyperbolic conservation laws in one dimensional space

$$u_t + f(u)_x = 0 \quad x \in [a, b], \tag{2.1}$$

which might yield discontinuous solutions even though the initial condition is smooth.

Given a grid

$$a = x_{\frac{1}{2}} < x_{\frac{3}{2}} < ... < x_{N-\frac{1}{2}} < x_{N+\frac{1}{2}} = b,$$

define

$$I_j = [x_{j-\frac{1}{2}}, x_{j+\frac{1}{2}}]$$

to be a cell with size $\Delta x_j = x_{j+\frac{1}{2}} - x_{j-\frac{1}{2}}$. For simplicity, we consider uniform meshes in the report. The cell average of a function $u(x)$ is denoted by

$$\bar{u}_j = \frac{1}{\Delta x_j} \int_{x_{j-\frac{1}{2}}}^{x_{j+\frac{1}{2}}} u(x) dx.$$

Integrating (2.1), we have

$$\int_{x_{j-\frac{1}{2}}}^{x_{j+\frac{1}{2}}} (u_t + f(u)_x)\ dx = 0,$$

$$\int_{x_{j-\frac{1}{2}}}^{x_{j+\frac{1}{2}}} u_t\ dx + \int_{x_{j-\frac{1}{2}}}^{x_{j+\frac{1}{2}}} f(u)_x\ dx = 0,$$

$$\Delta x_j (\bar{u}_j)_t + (f(u_{j+\frac{1}{2}}) - f(u_{j-\frac{1}{2}})) = 0.$$

$$(\bar{u}_j)_t + \frac{f(u_{j+\frac{1}{2}}) - f(u_{j-\frac{1}{2}})}{\Delta x_j} = 0.$$

With Euler forward time-discretization

$$\frac{\bar{u}_j^{n+1} - \bar{u}_j^n}{\Delta t} + \frac{f(u_{j+\frac{1}{2}}) - f(u_{j-\frac{1}{2}})}{\Delta x_j} = 0. \tag{2.2}$$

We can develop a finite volume scheme from (2.2) by reconstructing the $u_{j+\frac{1}{2}}$ at the cell interface by using

$$\bar{u}_j, \quad \text{with} \quad j = 1, 2, ..., N.$$

Notice the fact that the numerical approximation is piecewise constant, then $u_{j+\frac{1}{2}}$ is not well defined. Therefore, we need to introduce the numerical flux $\widehat{f}$ which depends on $u_{j+\frac{1}{2}}^-$ and $u_{j+\frac{1}{2}}^+$.

In general, we consider $\widehat{f}(u^-, u^+)$ to be a monotone numerical flux satisfying

(i) $\widehat{f}(u^-, u^+)$ is non decreasing in its first argument u^- and non increasing in its second argument u^+, denoted by $\widehat{f}(\uparrow, \downarrow)$;

(ii) $\widehat{f}(u^-, u^+)$ is consistent with the physical flux $f(u)$, i.e. $\widehat{f}(u, u) = f(u)$;

5

(iii) $\widehat{f}(u^-, u^+)$ is Lipschitz continuous with respect to both argument u^- and u^+.

Both $u^-_{j+\frac{1}{2}}$ and $u^+_{j+\frac{1}{2}}$ are obtained through the reconstruction procedure, with their stencil biased to the left and to the right, respectively.

Some monotone fluxes include

1. Lax-Friedrichs flux

$$\widehat{f}(u^-, u^+) = \frac{1}{2}(f(u^-) + f(u^+) - \alpha(u^+ - u^-)), \quad \alpha = \max_u |f'(u)|$$

2. Godunov flux

$$\widehat{f}(u^-, u^+) = \begin{cases} \min_{u^- \leq u \leq u^+} f(u), & \text{if } u^- < u^+, \\ \max_{u^+ \leq u \leq u^-} f(u), & \text{if } u^- \geq u^+. \end{cases}$$

Next, we will consider the general procedure of reconstruction for finite volume scheme. In order to reconstruct $u^-_{j+\frac{1}{2}}$, we need to select the *stencil* which is the collection of consecutive cells near $x_{j+\frac{1}{2}}$ including I_j. For example to reconstruct $u^-_{j+\frac{1}{2}}$ given $\bar{u}_{j-1}, \bar{u}_j$ and $\bar{u}_{j+1}$.

1. Find the unique polynomial of degree two $p(x)$ satisfying the three cell averages $\bar{u}_{j-1}, \bar{u}_j$ and $\bar{u}_{j+1}$ for three cells in the stencil, respectively:

$$\frac{1}{\Delta x} \int_{x_{j-\frac{3}{2}}}^{x_{j-\frac{1}{2}}} p(x) = \bar{u}_{j-1}, \tag{2.3}$$

$$\frac{1}{\Delta x} \int_{x_{j-\frac{1}{2}}}^{x_{j+\frac{1}{2}}} p(x) = \bar{u}_j, \tag{2.4}$$

$$\frac{1}{\Delta x} \int_{x_{j+\frac{1}{2}}}^{x_{j+\frac{3}{2}}} p(x) = \bar{u}_{j+1}. \tag{2.5}$$

2. Take the value $p(x_{j+\frac{1}{2}})$ as an approximate to $u^-_{j+\frac{1}{2}}$:

$$u^-_{j+\frac{1}{2}} = p(x_{j+\frac{1}{2}}).$$

3. From (2.3)-(2.5), we can write $p(x_{j+\frac{1}{2}})$ as a linear combination of the given cell averages $\bar{u}_{j-1}, \bar{u}_j$ and $\bar{u}_{j+1}$. For example,

$$u_{j+\frac{1}{2}}^- = -\frac{1}{6}\bar{u}_{j-1} + \frac{5}{6}\bar{u}_j + \frac{1}{3}\bar{u}_{j+1}.$$

This approximation is third order accurate.

For general, k order of accuracy, we can write

$$u_{j+\frac{1}{2}}^- = \sum_{i=0}^{k-1} c_{ri}\bar{u}_{j-r+i} \tag{2.6}$$

for some constant c_{ri}. Some of the c's are given in Table 2.1.

k	r	j=0	j=1	j=2
1	-1	1		
	0	1		
2	-1	3/2	-1/2	
	0	1/2	1/2	
	1	-1/2	3/2	
3	-1	11/6	-4/6	1/3
	0	1/3	5/6	-1/6
	1	-1/6	5/6	1/3
	2	1/3	-7/6	11/6

Table 2.1: The constant c_{ri} in (2.6).

7

2.2   WENO Scheme

We will consider the WENO reconstruction procedure. WENO is based on ENO which is uniformly high order accurate right up to the discontinuity and one suitable stencil is selected from several candidates by a local smoothness. However, WENO reconstruction can improve some properties of ENO that are:

(i) We can get the high-order of accuracy with the same set of candidate stencils: with k stencils we can obtain k-th order accurate ENO scheme while $2k - 1$-th order accurate WENO scheme.

(ii) We can have the neater programming because the logical *if* will not appear in the WENO to choose the stencil unlike ENO.

(iii) We can obtain a more robust scheme for some special problem. For example, with initial condition e^{-x}, the ENO procedure will select the unstable stencil to approximate the solution.

Next, we will explain the WENO reconstruction procedure. We use the numerical flux obtained from fixed stencil low order finite volume schemes to create a high order numerical flux and the numerical scheme will be oscillatory in the presence of shocks by the Godunov Theorem stated in [2].

The general procedure of a WENO reconstruction is the following:

1. Compute the approximation from several different sub-stencils. Suppose the k candidate stencils

$$S_r(j) = \{I_{j-r}, I_{j-r+1}, ..., I_{j-r+k-1}\}, \qquad r = 0, 1, .., k-1$$

provide k different reconstructions to the value $u^-_{j+\frac{1}{2}}$, from (2.6)

$$u^{(r)}_{j+\frac{1}{2}} = \sum_{i=0}^{k-1} c_{ri} \bar{u}_{j-r+i}.$$

2. Find the combination coefficients to have a convex combination of all $u_{j+\frac{1}{2}}^{(r)}$ to be a new approximation

$$u_{j+\frac{1}{2}}^{-} = \sum_{r=0}^{k-1} \omega_r u_{j+\frac{1}{2}}^{(r)},$$

which require

$$\omega_r \geq 0, \quad \sum_{r=0}^{k-1} \omega_r = 1$$

for stability and consistency.

If the function $u(x)$ is smooth in all of the candidate stencils, there are constants d_r called *linear weights* such that

$$u_{j+\frac{1}{2}}^{-} = \sum_{r=0}^{k-1} d_r u_{j+\frac{1}{2}}^{(r)} = u(x_{j+\frac{1}{2}}) + O(\Delta x^{2k-1})). \tag{2.7}$$

For instance, for $1 \leq k \leq 3$

$$k = 1: \ d_0 = 1$$
$$k = 2: \ d_0 = \frac{2}{3}, \ d_1 = \frac{1}{3}$$
$$k = 3: \ d_0 = \frac{3}{10}, \ d_1 = \frac{3}{5}, \ d_2 = \frac{1}{10}$$

Because of consistency,

$$d_r \geq 0, \quad \sum_{r=0}^{k-1} d_r = 1.$$

When the function $u(x)$ has a discontinuity in one or more of the stencils, the weights should be essentially 0, smooth function of the cell averages involved and computationally efficient. We use the *smoothness indicators*

$$\beta_r = \sum_{l=1}^{k-1} \int_{x_{j-\frac{1}{2}}}^{x_{j+\frac{1}{2}}} \Delta x^{2l-1} (\frac{\partial^l p_r(x)}{\partial^l x})^2 dx.$$

9

For example, for $k = 3$,

$$\beta_0 = \frac{13}{12}(\bar{u}_{j-2} - 2\bar{u}_{j-1} + \bar{u}_j)^2 + \frac{1}{4}(\bar{u}_{j-2} - 4\bar{u}_{j-1} + 3\bar{u}_j)^2$$

$$\beta_1 = \frac{13}{12}(\bar{u}_{j-1} - 2\bar{u}_j + \bar{u}_{j+1})^2 + \frac{1}{4}(\bar{u}_{j-1} - \bar{u}_{j+1})^2$$

$$\beta_2 = \frac{13}{12}(\bar{u}_j - 2\bar{u}_{j+1} + \bar{u}_{j+2})^2 + \frac{1}{4}(3\bar{u}_j - 4\bar{u}_{j+1} + \bar{u}_{j+2})^2.$$

Base on the indicator, we can construct the weights

$$\alpha_r = \frac{d_r}{(\varepsilon + \beta_r)^2}.$$

By taking $\varepsilon = 10^{-6}$ to avoid zero in the denominator.
Then *nonlinear weights* are defined by

$$\omega_r = \frac{\alpha_r}{\sum_{s=0}^{k-1} \alpha_s}, \quad r = 0, 1, ..., k-1.$$

We consider fifth order WENO as an example. The three stencils are:

$$S_0 = \{I_j, I_{j+1}, I_{j+2}\}, \quad S_1 = \{I_{j-1}, I_j, I_{j+1}\}, \quad S_2 = \{I_{j-2}, I_{j-1}, I_j\}$$

From (2.6), we have

$$u_{j+\frac{1}{2}}^{(0)} = \frac{1}{3}\bar{u}_j + \frac{5}{6}\bar{u}_{j+1} - \frac{1}{6}\bar{u}_{j+2},$$

$$u_{j+\frac{1}{2}}^{(1)} = -\frac{1}{6}\bar{u}_{j-1} + \frac{5}{6}\bar{u}_j + \frac{1}{3}\bar{u}_{j+1},$$

$$u_{j+\frac{1}{2}}^{(2)} = \frac{1}{3}\bar{u}_{j-2} - \frac{7}{6}\bar{u}_{j-1} + \frac{11}{6}\bar{u}_j.$$

If the function $u(x)$ is smooth in all three sub-stencils, then the three approximations $u_{j+\frac{1}{2}}^{(0)}, u_{j+\frac{1}{2}}^{(1)}$ and $u_{j+\frac{1}{2}}^{(2)}$ are all third order of accuracy and

$$\bar{u}_{j+\frac{1}{2}} = \frac{3}{10}u_{j+\frac{1}{2}}^{(0)} + \frac{3}{5}u_{j+\frac{1}{2}}^{(1)} + \frac{1}{10}u_{j+\frac{1}{2}}^{(2)}$$

would lead to a fifth order accurate linear scheme which is oscillatory.

Program method:

1. Set up:

   Define mesh size, time step, $\frac{\Delta t}{\Delta x}$, all parameters including c_{ri}.

2. Initial condition:

3. If (t<tend)

   1) Boundary condition
   2) Compute flux
   3) Compute weights
   4) Add them up to obtain the numerical flux
   5) Time integral

   e.g. strong stability preserving Runge-Kutta

$$u_t = L(u)$$
$$u^{(1)} = u^n + \Delta t L(u^n)$$
$$u^{(2)} = \frac{3}{4}u^n + \frac{1}{4}(u^{(1)} + \Delta t L(u^{(1)}))$$
$$u^{(n+1)} = \frac{1}{3}u^n + \frac{2}{3}(u^{(2)} + \Delta t L(u^{(1)}))$$

   $t = t + \Delta t$
   end if

4. Out put:

   Error table or figure.

Chapter 3

Numerical Experiments

In this section we will demonstrate some numerical experiments to test the accuracy of our code. Then we will consider the problem with singularities and find out the size of the pollution region.

3.1 Pollution Region

For partial differential equations with singularities, the numerical approximation may be oscillatory near the discontinuity which we refer to as the pollution region. We will demonstrate how to find the size of the pollution region numerically.

3.1.1 Algorithm

After we have obtained the numerical approximation, we can compute the size of pollution region which is assume to be $O(h^r)$. The way to find the value r, described in [5], is the following:

1. Compute a cumulative L^2- error e_m^l for each $m \geq 1$ and $l \geq 1$, where m is the number of intervals divided from original domain and l denote the l-th mesh with mesh size $h_l = (b-a)2^{-l+1}/1000$, for interval $[a, b]$ in considered problem.

2. Find out the boundary position m_l for each mesh:

   (a) Let $l = 1$. We can visually choose the error e_m^1 by choosing a suitable boundary position m_1. Find a position where its cumulative error differ to the next one significant. It should stay near the singularity point for this mesh.

   (b) Define the starting error $\Psi_{l+1} = e_{m_l}^l / (h_l/h_{l+1})^{k+0.95}$, where k is the degree of piecewise polynomials, and because of the mesh refinement in this test $h_l/h_{l+1} = 2$. Next, we visually scan e_m^{l+1} until the error $e_{m_{l+1}}^{l+1}$ pass below the starting error Ψ_{l+1}. Then we get the boundary position m_{l+1}.

   (c) Let $l = l + 1$, go back to step (b).

3. Use a least square procedure to find the slope s_2 in a linear equation

$$\ln d = s_2 \ln h + C$$

with the collect data (h_l, d_l). where d_l is the distance between the edge of the pollution region and the position of the singularity i.e. $y - m_l h_l$ with a singularity at y.

3.2 Numerical Experiments

3.2.1 Basic tests

In this part, we will test the performance of the Finite Volume Method(FVM) and WENO scheme about the order of accuracy.

Example 1 *Finite Volume Method(FVM) Accuracy test*

We test with accuracy of the third order FVM with a middle stencil for the following problem

$$\begin{cases} u_t + u_x & = 0 \\ u(x,0) & = \sin x, \quad x \in [0, 2\pi] \\ u(0,t) & = u(2\pi, t) \end{cases}$$

we consider the L^2 errors between the numerical and exact solutions, and the order of accuracy at $t = 0.5$ by taking $N = 10, 20, 40, 80, 160, 320$. The time step is taken as $dt = 0.01dx$. The results are listed in Table 3.1.

N	L^2 error	Order of accuracy
10	8.73131393915629E-03	-
20	1.13616582593133E-03	2.94202536061148
40	1.43416960668578E-04	2.98588586060677
80	1.79142287324152E-05	3.00103781190167
160	2.23710649361984E-06	3.00140009186039
320	2.79679976183875E-07	2.99978506284488

Table 3.1: L^2 error and order of accuracy for Example 1 with the third order FVM with a middle stencil at $T = 0.5$.

Figure 3.1: The numerical approximation for Example 1 at $T = 0.5$.

Example 2 *WENO Accuracy test*

We test with accuracy of the fifth order WENO scheme with a nonlinear weights for the following problem

$$
\begin{cases}
u_t + u_x & = 0 \\
u(x, 0) & = \sin x, \quad x \in [0, 2\pi] \\
u(0, t) & = u(2\pi, t)
\end{cases}
$$

we consider the L^2 errors between the numerical and exact solutions, and the order of accuracy at $t = 1$ by taking $N = 10, 20, 40, 80, 160, 320$. The time step is taken as $dt = 0.01dx$. The results are listed in Table 3.2.

15

N	L^2 error	Order of accuracy
10	1.93115975623156E-02	-
20	7.55713058465938E-04	4.67548515443402
40	2.20517393082530E-05	5.09887419582036
80	6.53821036834840E-07	5.07585284425216
160	1.97989050745567E-08	5.04540324364396
320	6.09991978729030E-10	5.02048656624585

Table 3.2: L^2 error and order of accuracy for Example 2 with the fifth order WENO scheme with a nonlinear weights at $T = 1$.

3.2.2 Pollution Region experiments

In this part we consider the problem with singularities and find out the size of the pollution region.

Example 3 *Finite Volume Method(FVM)*
We consider the third order FVM with a middle stencil for the following problem

$$\begin{cases} u_t + u_x & = 0 \\ u(x,0) & = \sin x, \quad x \in [0, 2\pi] \\ u(0,t) & = u(2\pi, t) \end{cases}$$

we consider the above problem with a single discontinuity at $x = 0.625$, we will find the L^2 errors between the numerical and exact solutions at final time $T = 0.25$ where the discontinuity moves to $x = 0.875$. The time step is taken as $dt = 0.01dx$. By taking the l-th mesh with mesh size $h_l = (2\pi)2^{-l+1}/1000$, $l = 1, 2, ..., 8$ we find the edge of pollution region is at the m_l-th cell. The results are listed in Table 3.3.

Figure 3.2: The numerical approximation for Example 2 at $T = 1$.

l	1	2	3	4	5	6	7	8
m_l	125	255	525	1071	2171	4382	8816	17701

Table 3.3: The numerical positions of the boundaries of the pollution region at the l-th mesh for Example 3.

Next we compute the slope s_2 in a linear equation $\ln d = s_2 \ln h + C$ by least square method with the collect data $(h_l, 0.875 - m_l h_l)$. We obtain $s_2 = 0.5805$. It is shown that the pollution region size is near the order $O(h^{1/2})$. So, it lead to conclusion that the size of pollution region is sharp for using third order FVM with middle stencils.
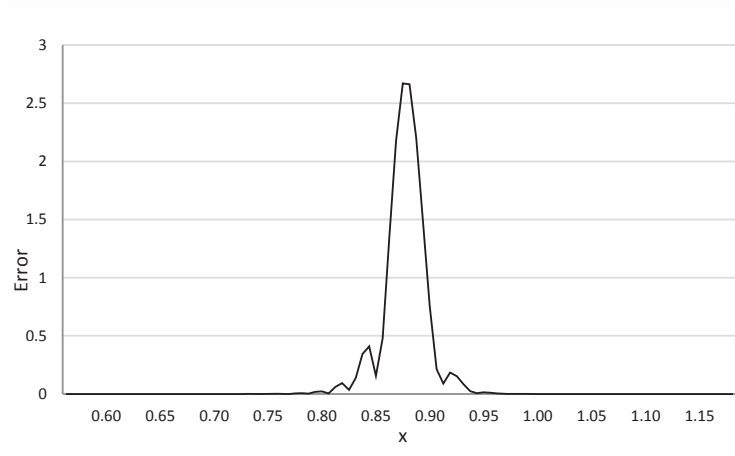
Figure 3.3: The error in a neighborhood of singularity point for the broadest mesh for Example 3.

Example 4 *(WENO)*

We consider the fifth order WENO scheme with a nonlinear weights for the following problem

$$\begin{cases} u_t + u_x & = 0 \\ u(x,0) & = \sin x, \quad x \in [0, 2\pi] \\ u(0,t) & = u(2\pi, t) \end{cases}$$

We follow the same way discussed in Example 3 to find m_l. The results are listed in Table 3.4.

18

l	1	2	3	4	5
m_l	116	244	510	1052	2148

Table 3.4: The numerical positions of the boundaries of the pollution region at the l-th mesh for Example 4.

Then we compute the slope s_2 in a linear equation $\ln d = s_2 \ln h + C$ by least square method with the collect data $(h_l, 0.875 - m_l h_l)$. We obtain $s_2 = 0.5614$. It is shown that the pollution region size is near the order $O(h^{1/2})$. Then, it can conclude that the pollution region size using fifth order WENO with a nonlinear weights is sharp.
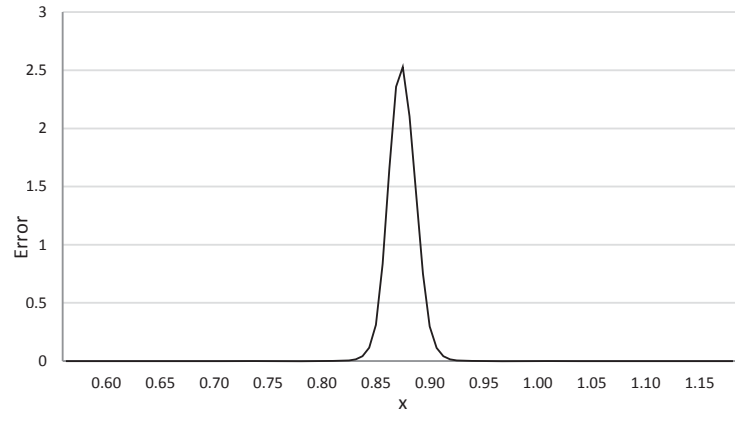

Figure 3.4: The error in a neighborhood of singularity point for the broadest mesh for Example 4.

Chapter 4

Conclusions and Future works

4.1　Conclusions

The pollution region size of hyperbolic conservation law with δ-singularities at $x = 0.875$ using third order FVM with middle stencils and fifth order WENO with a nonlinear weights is 0.5805 and 0.5614, respectively which are similar to $O(h^{1/2})$. According to the work in [5], we might conclude that the size of pollution region is sharp.

4.2　Future works

For a future work, we might study the hyperbolic conservation law with δ-singularities to find a pollution region size with the others method. Moreover, we can study a nonlinear partial differential equations. For instance, hyperbolic conservation law with $f(u) = \frac{u^2}{2}$, with δ-singularities and use WENO or discontinuous Galerkin (DG) method to find a size of pollution region such as the following problem

Problem 1 Consider the fifth order WENO scheme with a nonlinear weights for the following problem

$$
\begin{cases}
u_t + \left(\frac{u^2}{2}\right)_x & = 0 \\
u(x,0) & = \sin x + \frac{1}{2}, \quad x \in [0, 2\pi] \\
u(0,t) & = u(2\pi, t)
\end{cases}
$$

considering with a single discontinuity at some $y \in [0, 2\pi]$, at final time T.

Problem 2 Consider the second or third order DG scheme with Godunov flux and Lax-Fridrichs flux for the following problem

$$
\begin{cases}
u_t + \left(\frac{u^2}{2}\right)_x & = 0 \\
u(x,0) & = \sin x + \frac{1}{2}, \quad x \in [0, 2\pi] \\
u(0,t) & = u(2\pi, t)
\end{cases}
$$

at final time $T = 2$.

Bibliography

[1] A. Bressan, *Mathematics of Complexity and Dynamical Systems: Hyperbolic Conservation Laws*, Springer New York (2011), pp. 729-731.

[2] H. Im, *Lecture Notes on Computational Fluid Dynamics - I*, Department of Mechanical Engineering, University of Michigan (2001), ch. 9.

[3] C. W. Shu, *Essentially Non-Oscillatory and Weighted Essentially Non-Oscillatory Schemes for Hyperbolic Conservation Laws*, Institute for Computer Applications in Science and Engineering NASA Langley Research Center Hampton, VA, (1997), pp. 3-20.

[4] C. W. Shu, *Numerical Methods for Convection Dominated Partial Differential Equations*, Mathematics Department Tulane University, Clifford Lectures, (2013), ch 1.

[5] Q. Zhang and C. W. Shu, *Error estimates for the third order explicit Runge-Kutta discontinuous Galerkin method for a linear hyperbolic equation in one-dimension with discontinuous initial data*, Numerische Mathematik (2014), pp. 703-740.